Support Information

A highly efficient lanthanide coordination polymer luminescent material for multi–task detection of environmental pollutants

Contents

spectrum for ccpcTb.

Fig. S22 Energy profile diagram of ligand (H_3ccpc) and NACs with calculated HOMO and LUMO energies by DFT.

Table S1. Selected bond lengths (Å) for ccpcTb.

Table S2. Hydrogen bonds for ccpcTb lengths (Å) and angles (˚).

Table S3. Fluorescence intensity of the blank samples.

S1 Experimental section

Materials and Method. All materials are commercially available and were used without any further purification. Fourier-transform infrared spectra (FT-IR) are performed by using Mattson 7000 FT-IR Spectrometer with KBr Pellets (4000–400 cm^{-1}). ^1H NMR spectra were obtained by AVANCE III 400M Spectrometer. Elemental analyses (EA) for C, H, and N were performed in a Vario Macro CN microanalyzer. Thermogravimetric analysis (TGA) was carried out on Netzsch STA2500 Thermal Analyzer (heating rate = 10 °C/min) under N_2 atmosphere in the temperature range of 25–800°C. Scanning electron microscopy (SEM) was performed using a Hitachi S-3400N working at 20 kV. The UV-visible absorption spectra were obtained on the U-2910 UV–Vis spectrophotometer. Powder X-ray diffraction (PXRD) patterns were performed in the range of 5–50° by X'Pert powder diffractometer with Cu-Kα (λ = 1.5406 Å) radiation at room temperature. High-resolution mass spectra (HRMS) were recorded on an HR-ESI-MS from SCIE UPLC-Q-TOF (X 500R) Time of Flight (TOF analyzer). Luminescence spectra were recorded on FluoroMax Plus of HORIBA Scientific. The absolute emission quantum yield (QY) values were measured at RT using an Edinburgh quantum yield measurement system, equipped with a 150 W xenon lamp coupled to a monochromator for wavelength discrimination, an integrating sphere as the sample chamber, and a multichannel analyzer for signal detection. PL decays were recorded using an Edinburgh FLS980 steady state fluorimeter with a time-correlated single-photon counting (TCSPC) spectrometer and a pulsed xenon lamp as the excitation source.

X-ray Crystallography. Single crystal of **ccpcTb** suitable for X-ray analysis was obtained directly from the above preparations. The data of the **ccpcTb** were collected at room temperature on a Bruker Smart Apex2 CCD diffractometer with Mo Kα radiation (λ = 0.71073 Å) [1]. The data were integrated using the Siemens SAINT program [2]. With the intensities corrected for Lorentz factor, polarization, air absorption, and the absorption due to variation in the path length through the detector faceplate. Empirical absorption and extinction corrections were applied [3]. The structure of **ccpcTb** was solved by direct methods and then refined on the basis of F^2 with a full-matrix least-squares technique using the SHELXL crystallographic software package [4,5]. All the non-hydrogen atoms were refined anisotropically. The hydrogen

atoms were fixed at calculated positions, and afterward, refined as riding atoms using isotropic displacement parameters. Important crystallographic data are shown in Table S1. Some bond lengths and bond angles of **ccpcTb** are listed in Table S2. Hydrogen-bonding geometries of **ccpcTb** are listed in Table S3. CCDC reference numbers: 2255509.

Computational methodology and details

In this work, density functional theory (DFT) method based on Becke's three-parameter hybrid functional combined with the Lee-Yang-Parr correlation function (B3LYP) approach at level of 6-31G(d) basis sets was employed to optimize the configurations of H3ccpc ligand and 2,4,6-trinitrophenol in ground state, followed by frequency and energy calculations. In addition, the molecular structure of the first excited singlet of H3ccpc ligand was optimized by the time-dependent density functional theory (TD-DFT) at the B3LYP/6-31G (d, p) level. The excitation energies of the first excited singlet and the first excited triplet were also calculated using TD-DFT at the B3LYP/6-31G (d, p) level on the basis of configuration optimization. All theoretical calculations were carried out using the Gaussian 09 software package.[6].

Luminescence sensing experiments

Sensing environmental pollutants included twelve metal cations ($M(NO_3)_x$ (M^{x+} = K^+, Na^+, Zn^{2+}, Ni^{2+}, Co^{2+}, Cu^{2+}, Cd^{2+}, Mg^{2+}, Pb^{2+}, Al^{3+}, Cr^{3+}, Fe^{3+}) aqueous solution, ten anions (Na_nX, X = F^-, Br^-, I^-, NO_2^-, NO_3^-, BrO_3^-, Ac^-, CO_3^{2-}, SO_4^{2-}, $Cr_2O_7^{2-}$) aqueous solution and seven NACs (2,4,6-trinitrophenylphenol, 2-nitrotoluene, 3-nitrotoluene, 4-nitrotoluene, *p*-nitrophenol, 2,4-dinitrotoluene and nitrobenzene) methanol solution. For selective experiments, the ccpcTb dispersed solution (2 mg/mL, 1 mL) was added into a solution of testing (2 mM, 1 mL), respectively, then the luminescence intensity of mixture solution was examined. The luminescence intensity of **ccpcTb** solution showed different degrees of weakening by the introduced different sensing material solution. For titration experiment, the analyte solution was gradually added into the 2 mL dispersed solution of **ccpcTb** (2 mg/mL). The luminescence spectra of all mixture solutions were examined at 265 nm excitation by fluorescence spectroscopy (HORIBA FluoroMax Plus).

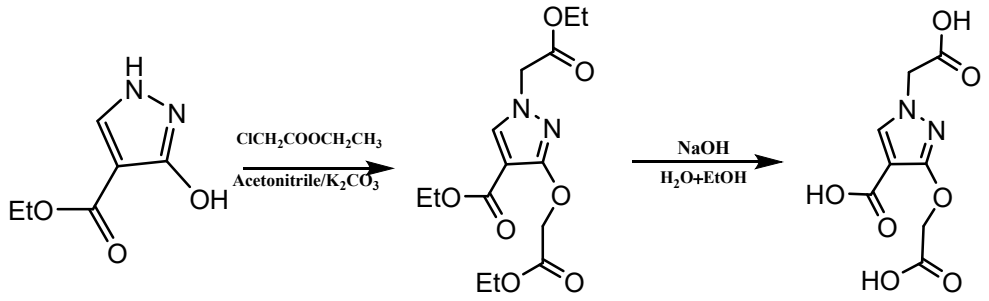

Scheme S1 Synthesis of 3-(carboxymethoxy)-1-(carboxymethyl)-pyrazole-4-carboxylic acid (H_3ccpc).

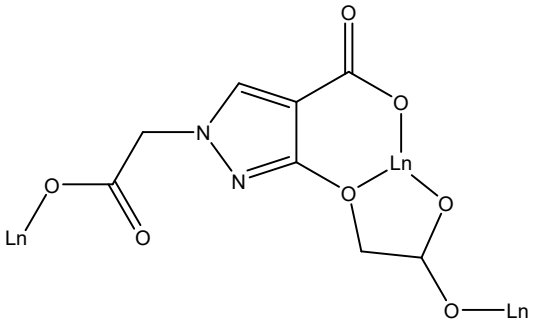

Scheme S2 Coordination mode of ccpcTb.

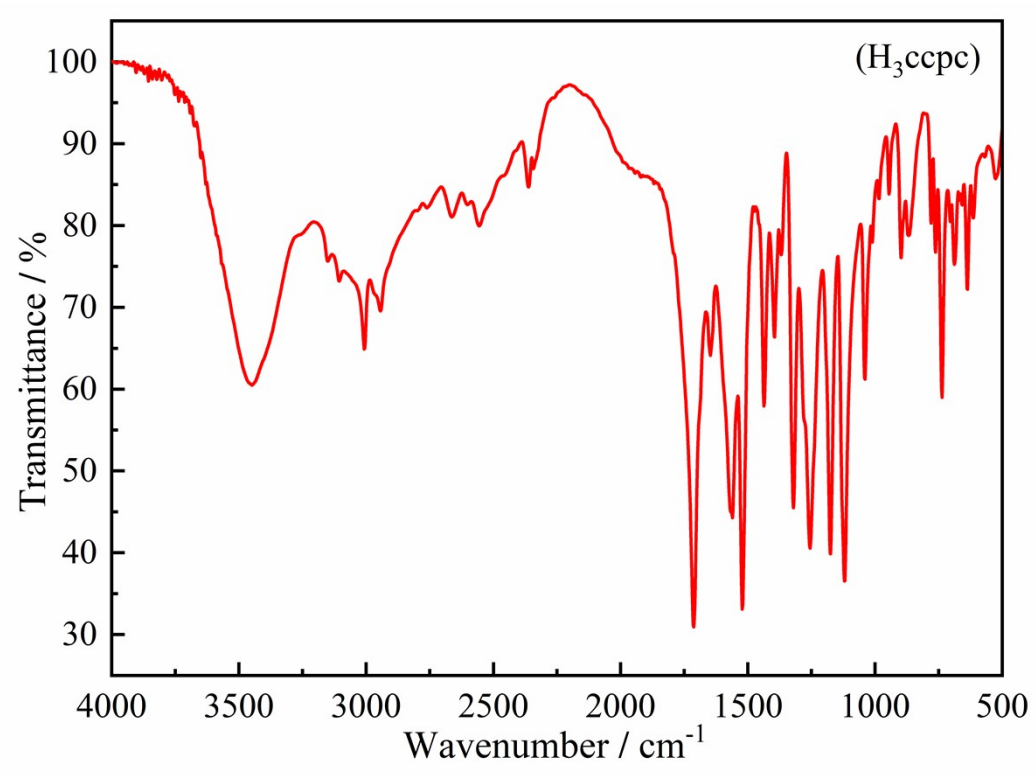

Fig. S1 FT-IR spectrum of H_3ccpc.

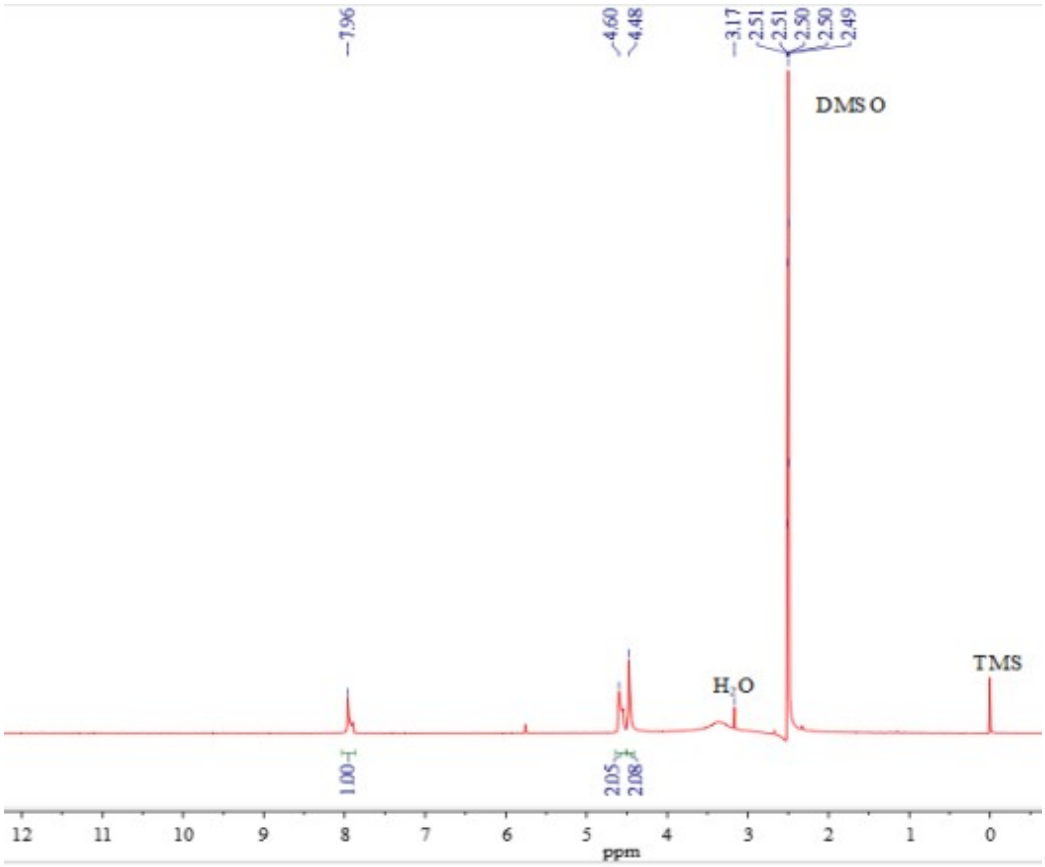

Fig. S2 ^{1}H NMR spectrum of H_3ccpc.

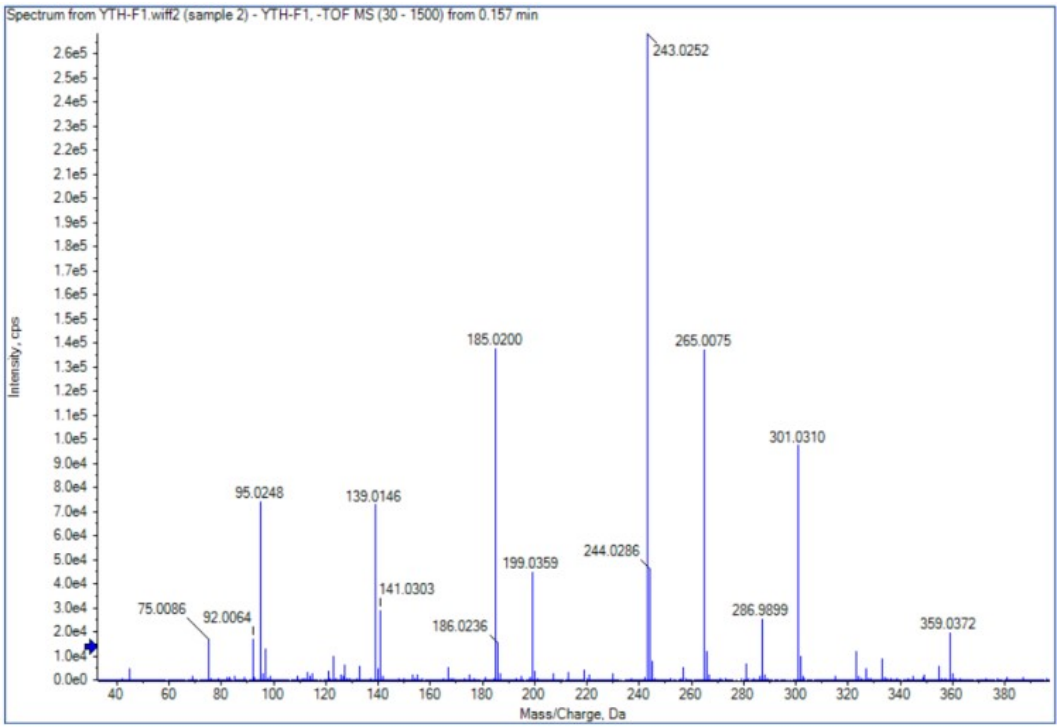

Fig. S3 High resolution mass spectrum of H_3ccpc.

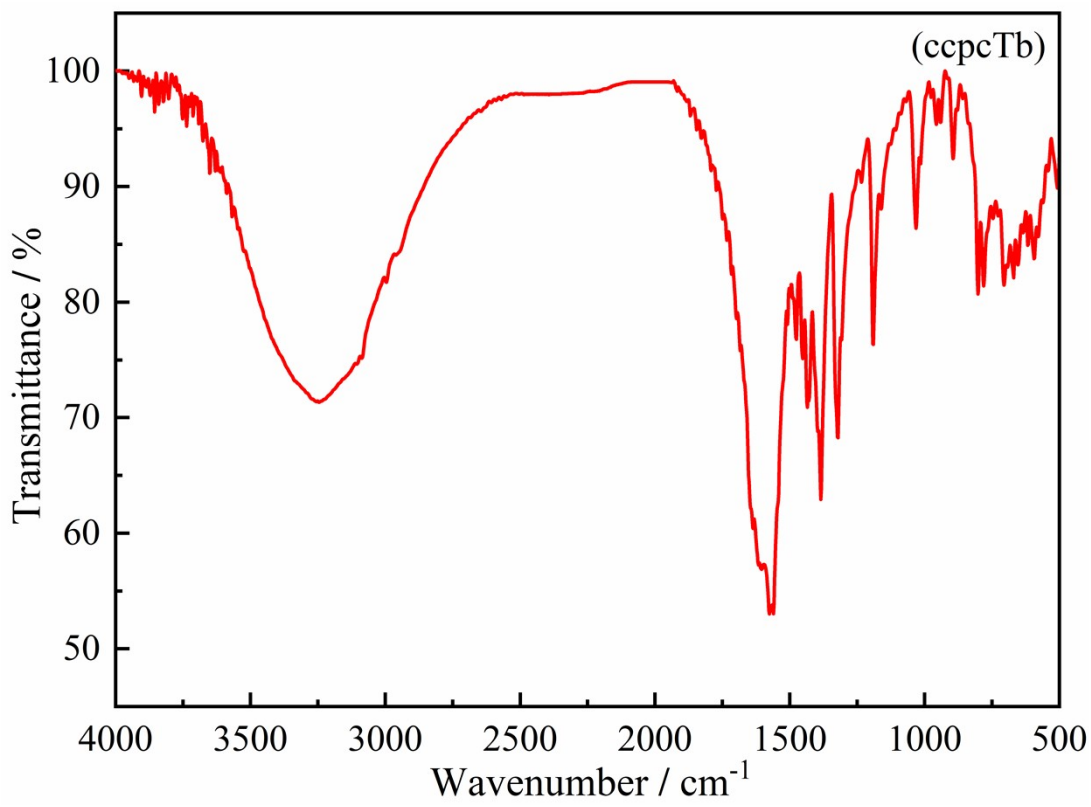

Fig. S4 FT-IR spectrum of ccpcTb.

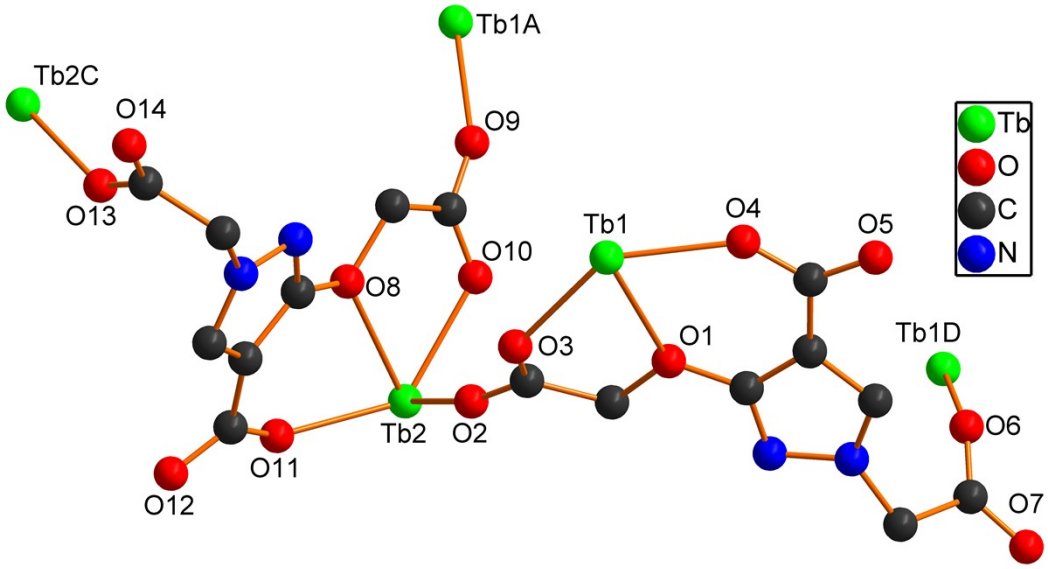

Fig. S5 Organic ligand H_3ccpc links two Tb^{3+} ions.

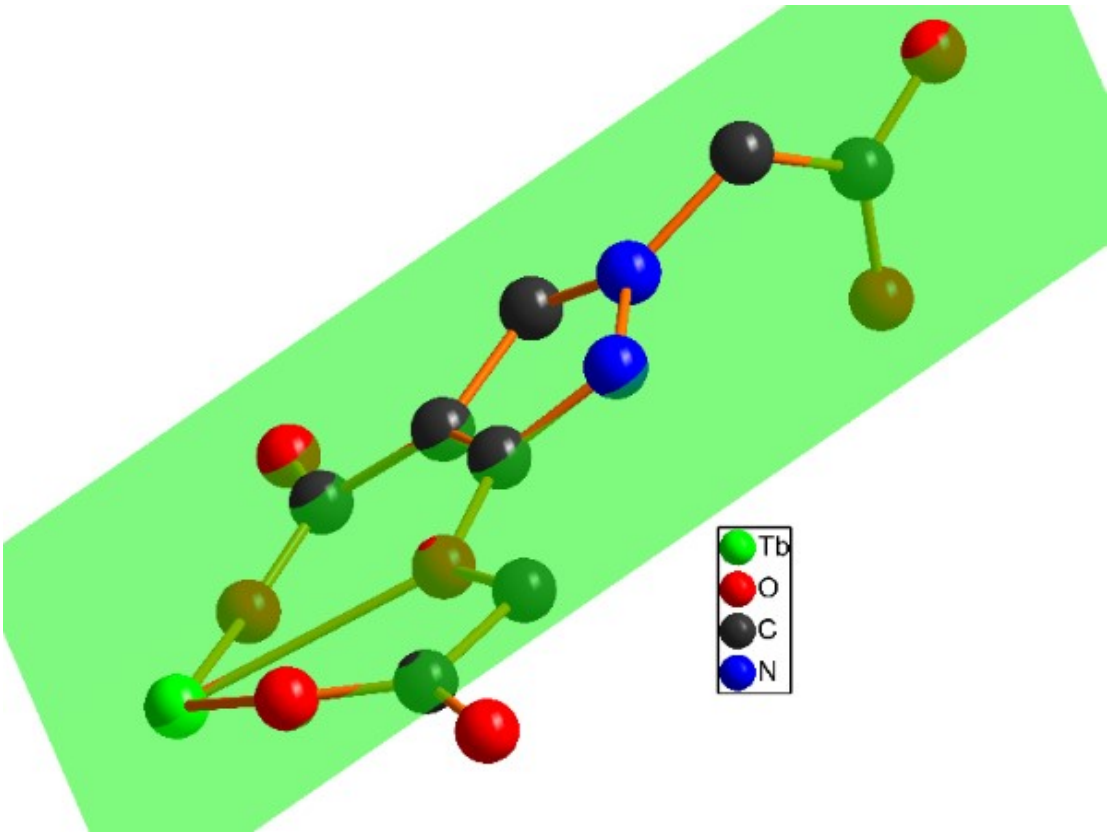

Fig. S6 Pyrazole ring and two coordination rings in the same plane.

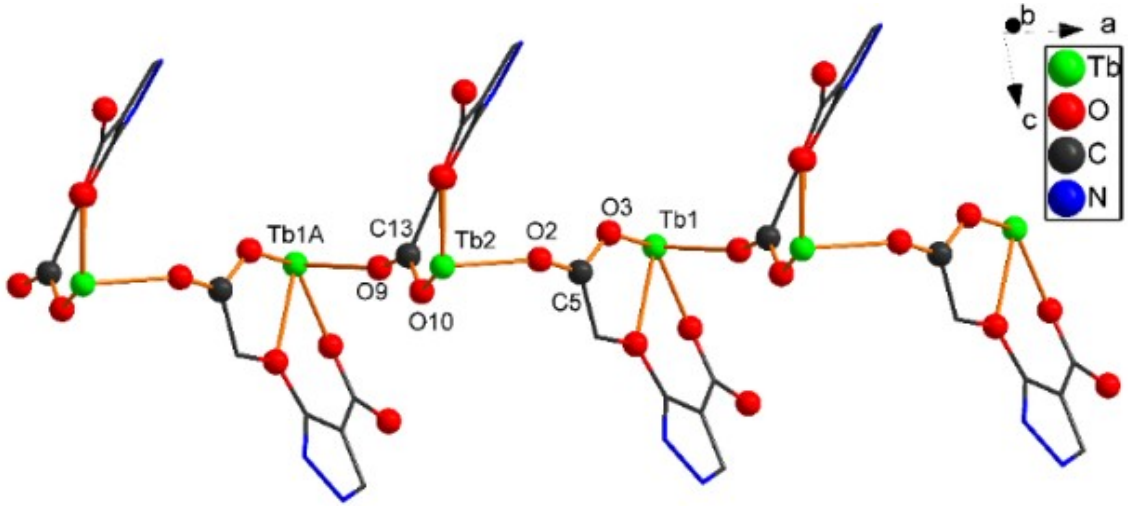

Fig. S7 Inorganic chain of Tb1 and Tb2 along the a-axis.

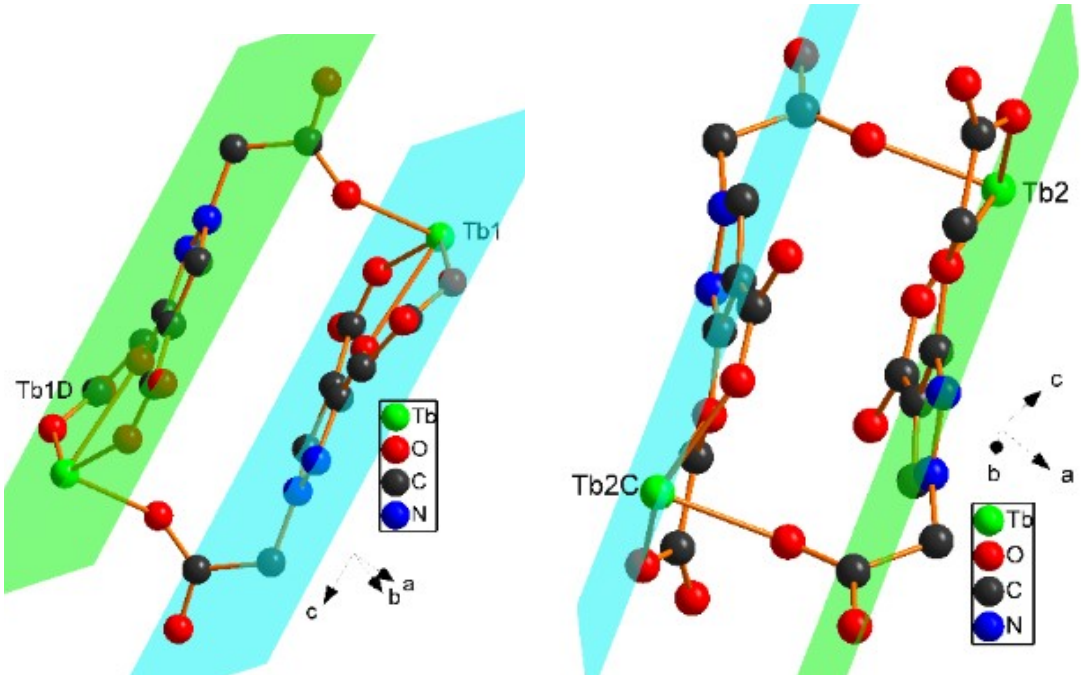

Fig. S8 Two coordination rings in the same plane.

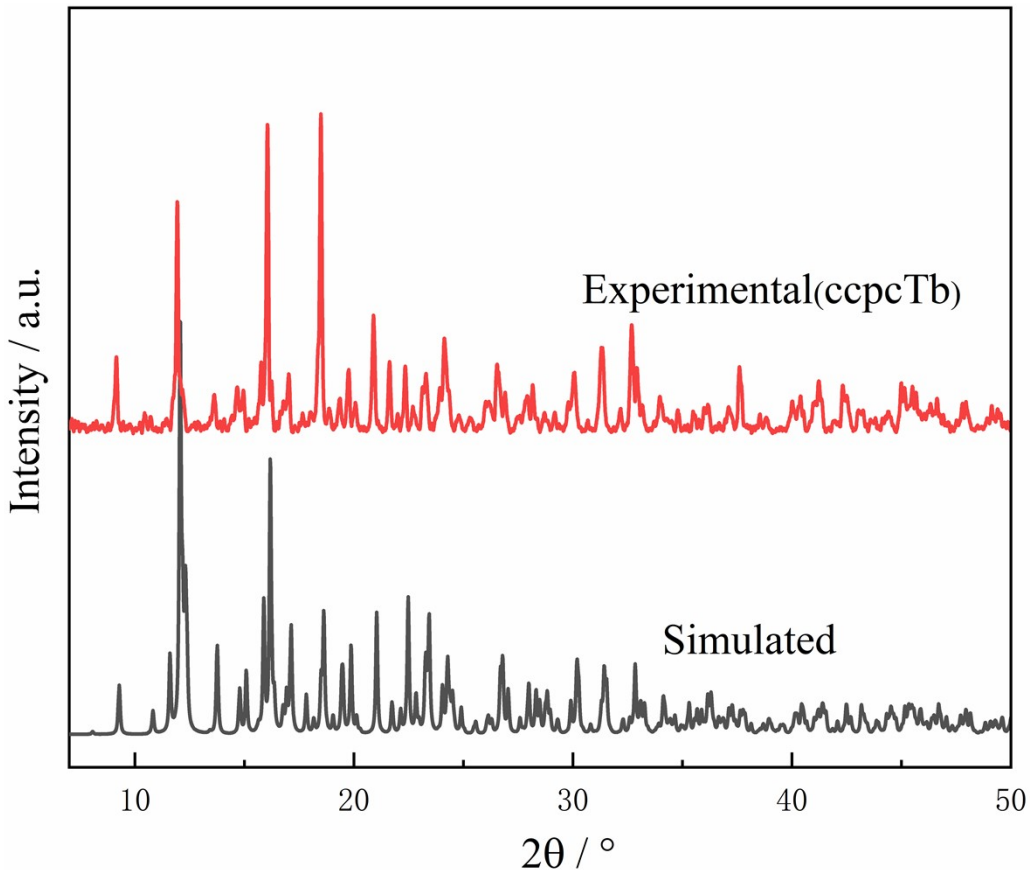

Fig. S9 Experimental and simulated PXRD patterns for ccpcTb.

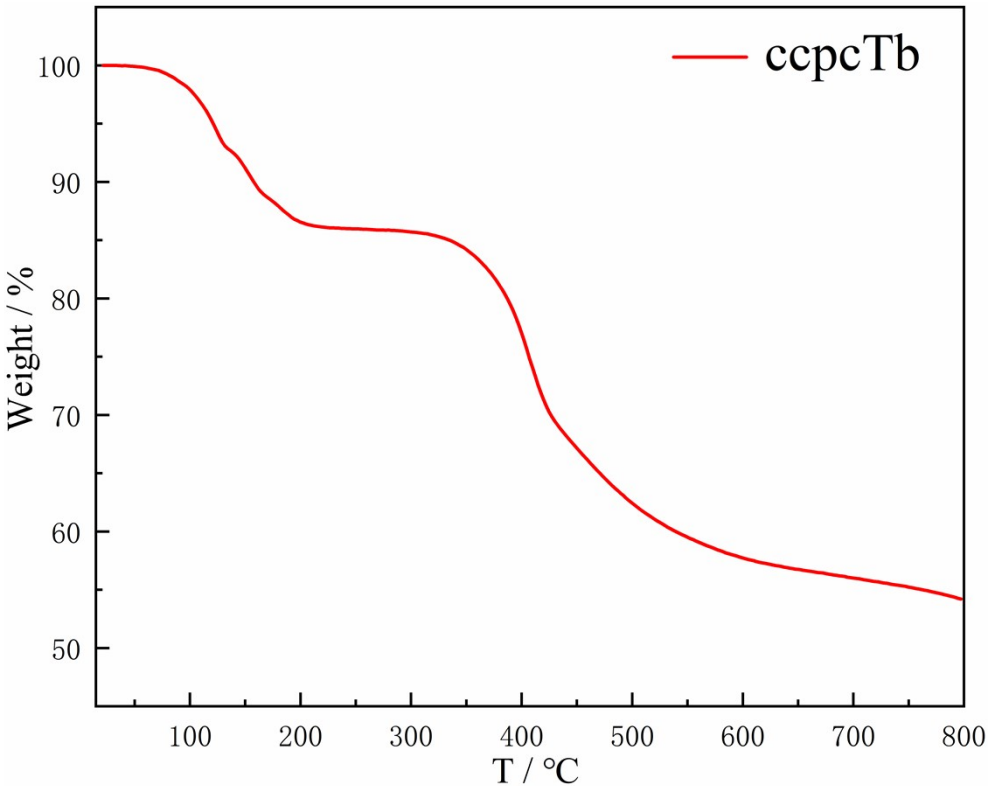

Fig. S10 TGA curve for ccpcTb.

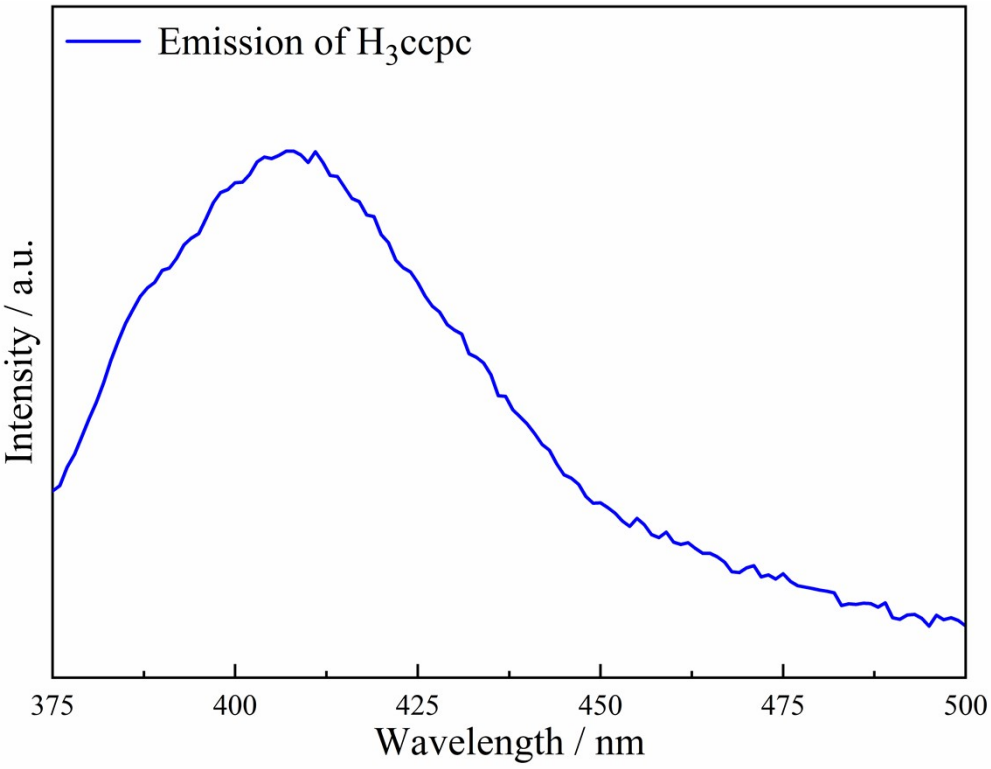

Fig. S11 Solid state fluorescence emission spectrum of H_3ccpc.

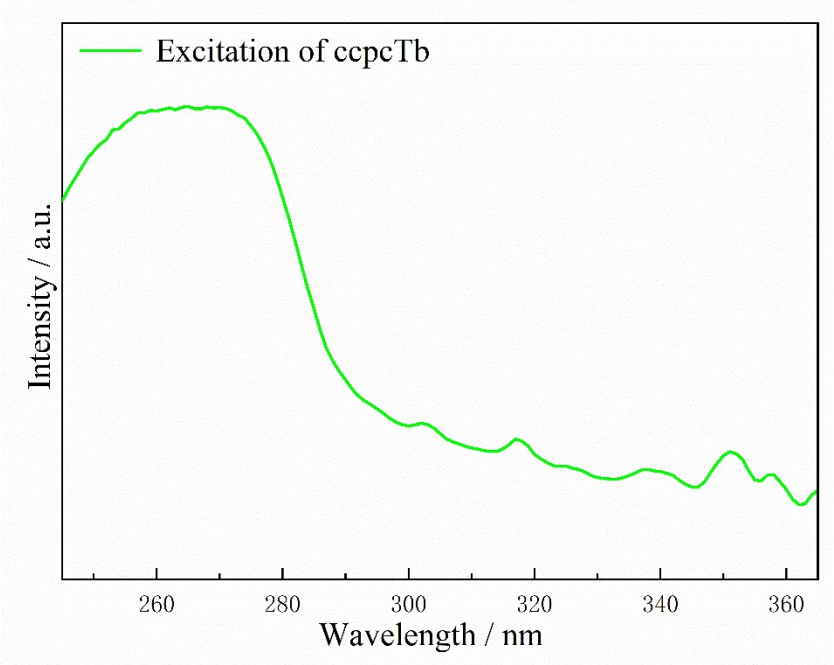

Fig. S12 Excitation spectrum of ccpcTb monitored at 542 nm.

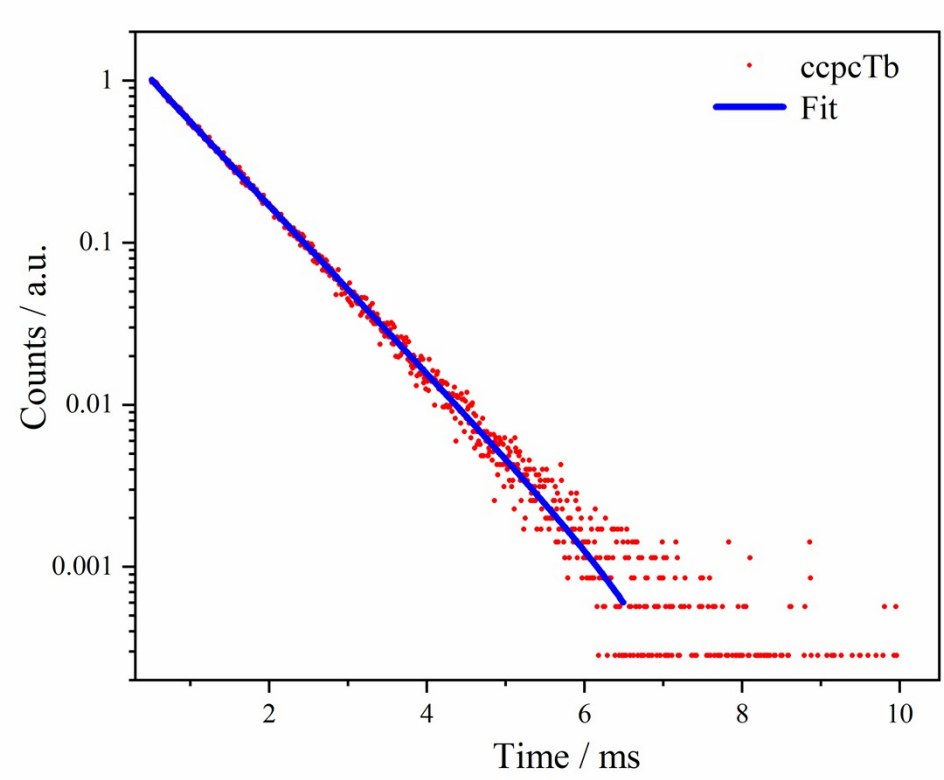

Fig. S13 Luminescence decay curve of ccpcTb.

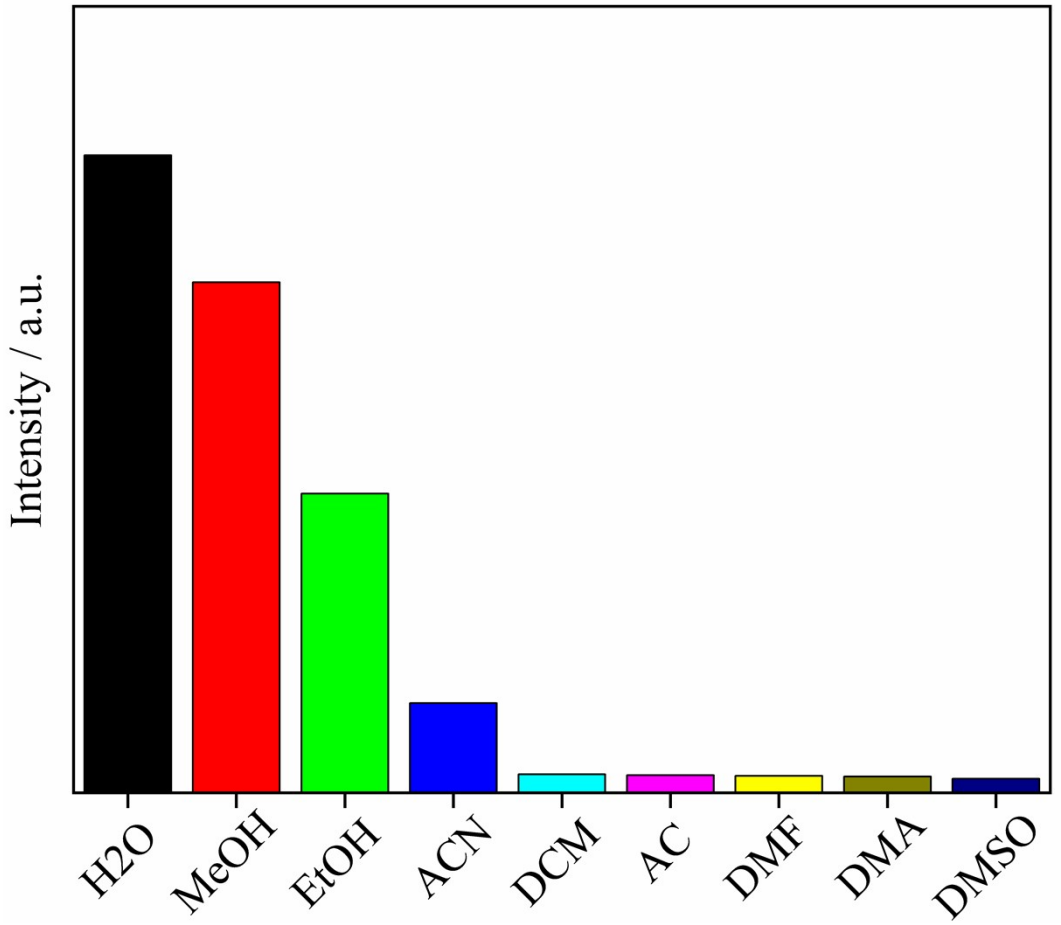

Fig. S14 Fluorescence intensities of ccpcTb in different solvents at 542 nm (λ_{ex} = 265 nm).

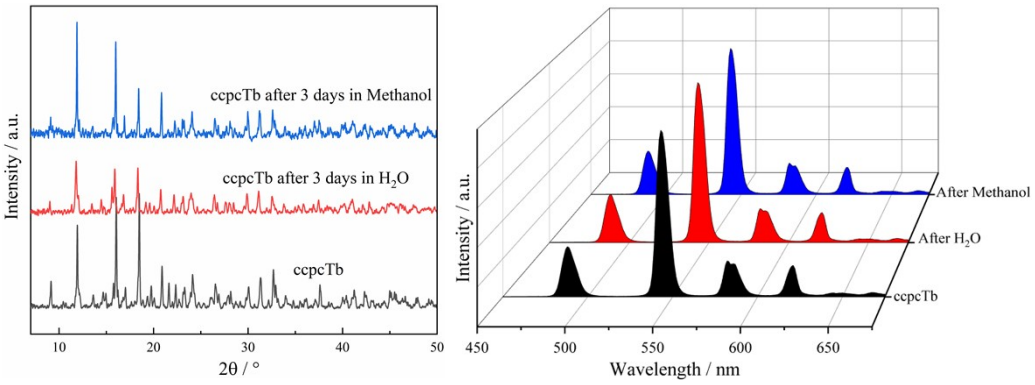

Fig. S15 PXRD patterns and emission spectra of ccpcTb after immersed in water and methanol for three days.

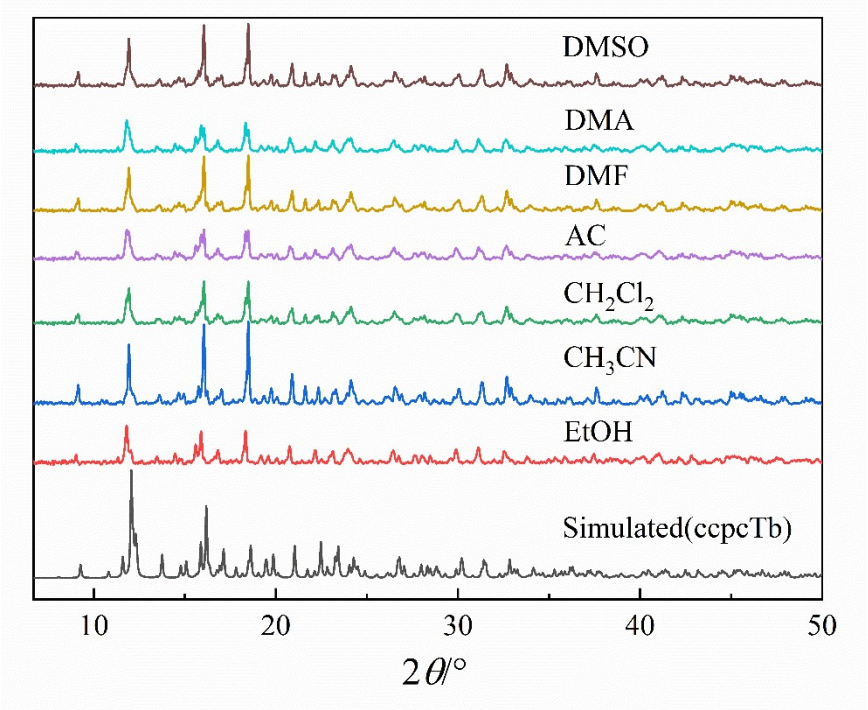

Fig. S16 PXRD patterns of ccpcTb after immersed in different solvents.

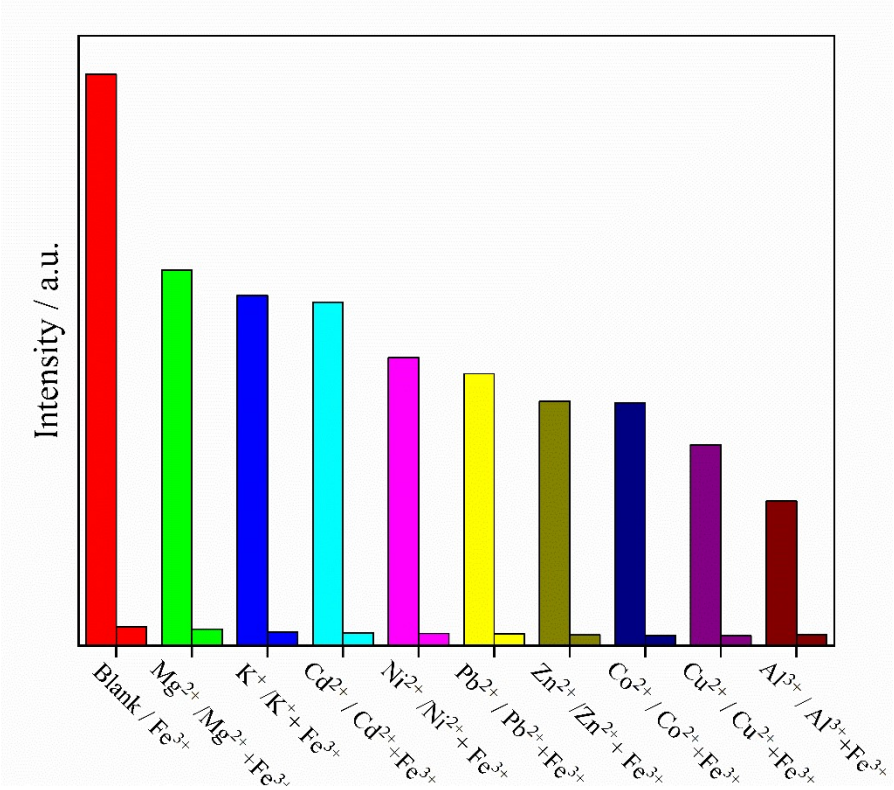

Fig. S17 Anti-interference experiment of ccpcTb for detection of Fe^{3+} ion.

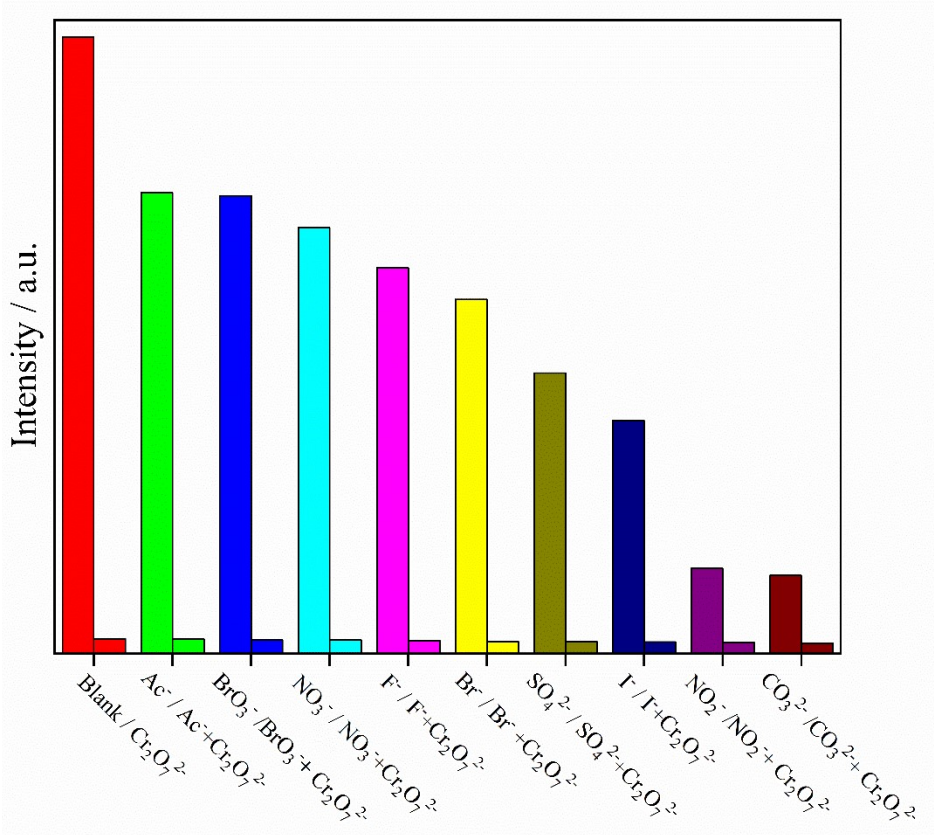

Fig. S18 Anti-interference experiment of ccpcTb for detection of $Cr_2O_7^{2-}$ anion.

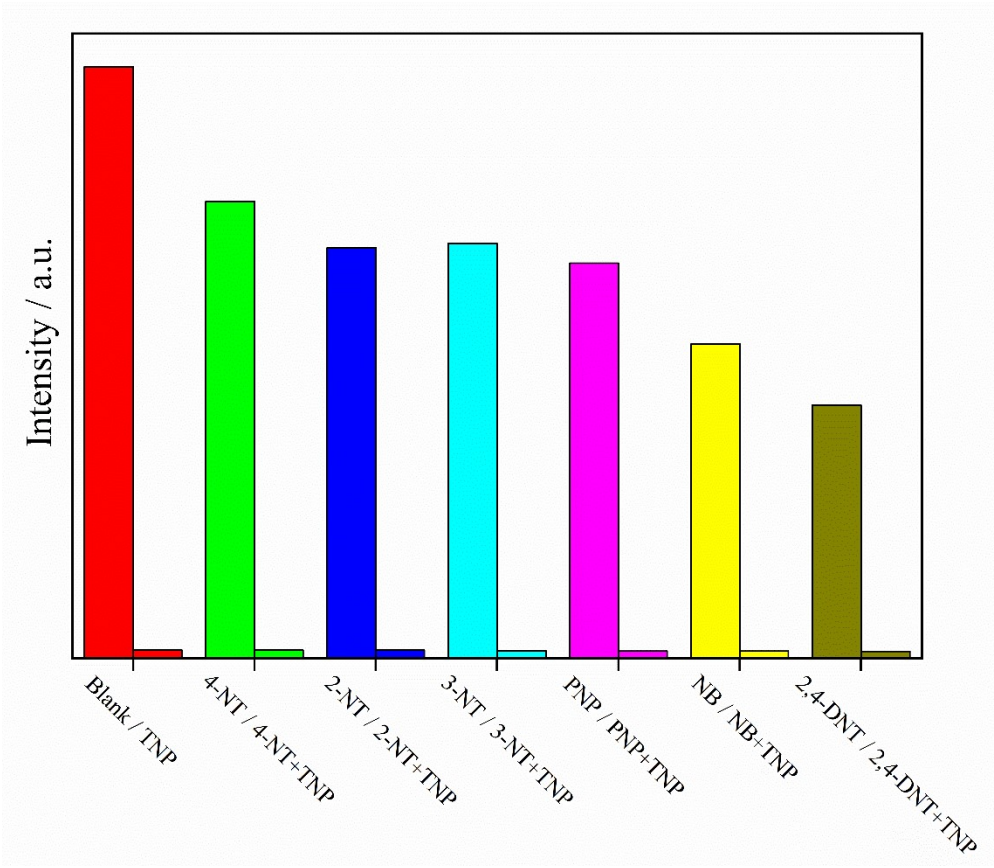

Fig. S19 Anti-interference experiment of ccpcTb for detection of TNP.

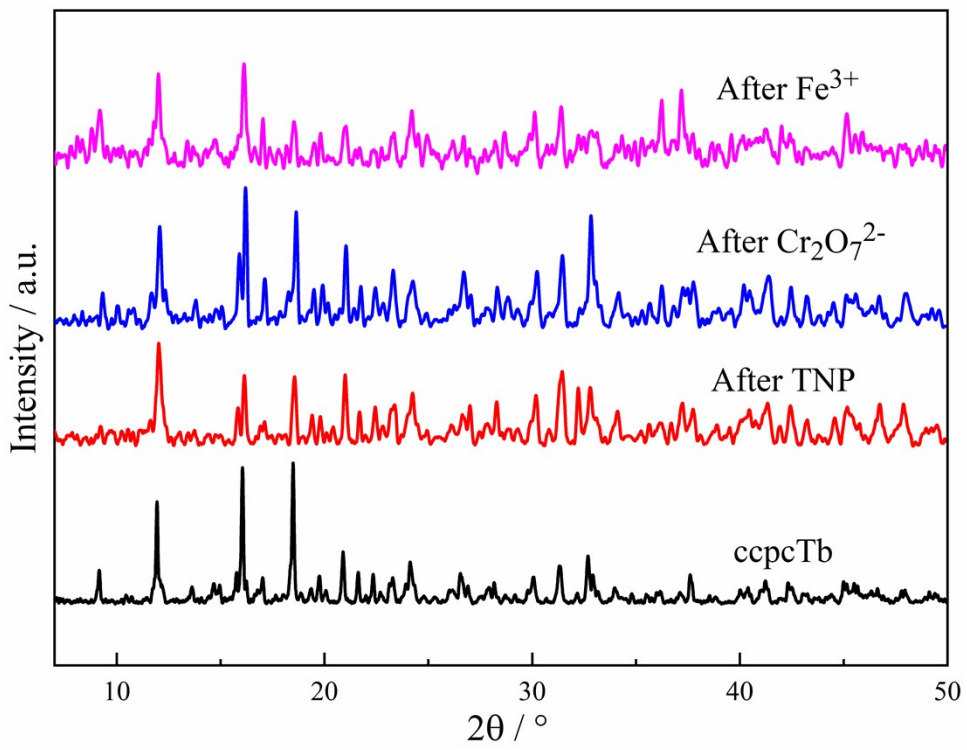

Fig. S20 PXRD patterns before and after Fe^{3+}, $Cr_2O_7^{2-}$ and TNP sensing.

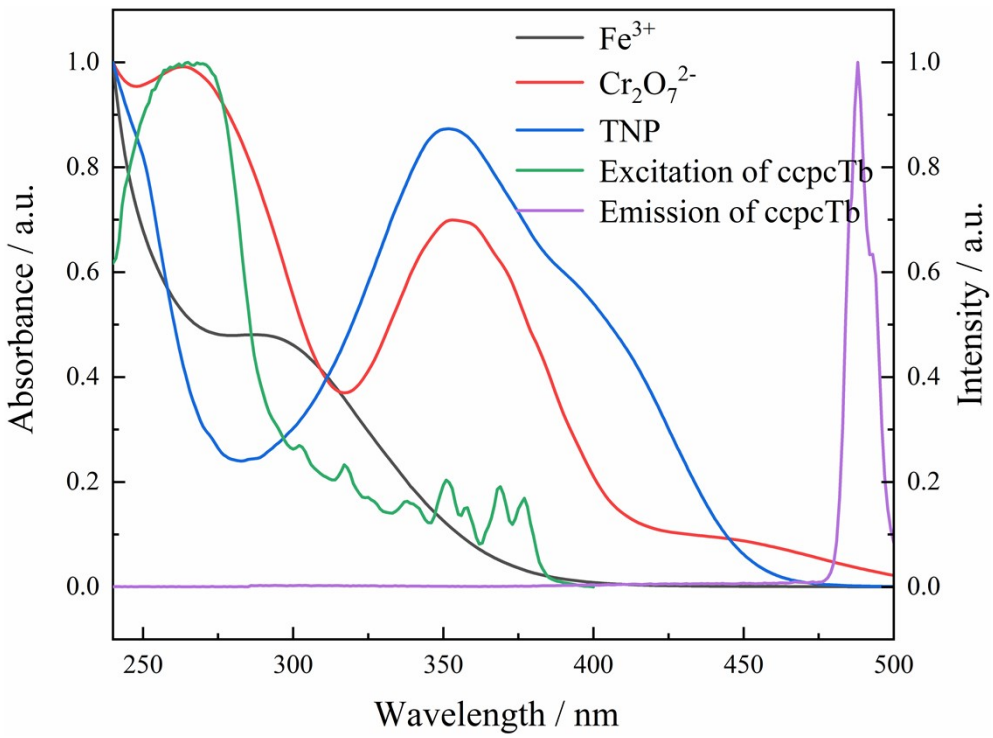

Fig. S21 UV–Vis absorption spectra of Fe^{3+}, $Cr_2O_7^{2-}$, TNP and the PL spectrum for ccpcTb.

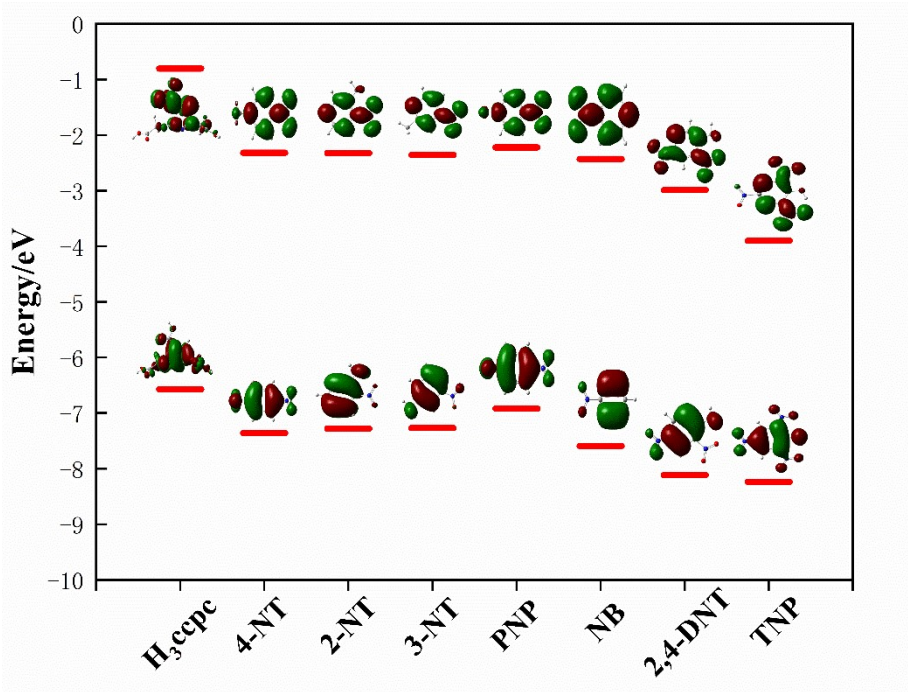

Fig. S22 Energy profile diagram of ligand H_3ccpc and NACs with calculated HOMO and LUMO energies by DFT.

Table S1 Selected bond lengths (Å) for ccpcTb.

	ccpcTb
Tb1–O1	2.658(3)
Tb1–O1W	2.362(4)
Tb1–O2W	2.472(4)
Tb1–O3	2.384(3)
Tb –O3W	2.338(3)
Tb1–O4	2.258(4)
Tb1–O9B	2.338(4)
Tb1–O6D	2.282(4)
Tb2–O2	2.318(4)
Tb2–O4W	2.360(4)
Tb2–O5W	2.370(4)
Tb2–O6W	2.413(4)
Tb2–O8	2.584(3)
Tb2–O10	2.350(3)
Tb2–O11	2.302(3)
Tb2–O13C	2.300(4)

Symmetry code: B: 1+x,y,z C: –x,1–y,–z D: 1–x,–y,1–z

Table S2 Hydrogen bonds for ccpcTb lengths (Å) and angles (˚).

DH···A	DH	H···A	D···A	DH···A
O1W–H1WA···O7	0.85	2.00	2.669(6)	135
O1W–H1WB ···O12	0.85	2.28	2.766(6)	116
O2W–H2WA···O6	0.85	2.51	2.791(6)	100
O2W–H2WB···O11	0.85	2.11	2.959(5)	176
O3W–H3WA···O3	0.85	2.55	2.913(5)	107
O3W–H3WA···O7W	0.85	2.37	2.750(6)	108
O3W–H2WB···O12	0.85	1.85	2.658(6)	160
O4W–H4WA···O8W	0.85	2.39	2.98(2)	127
O4W–H4WA···O4W	0.85	2.58	2.916(8)	105
O4W–H4WB···O10	0.85	2.51	2.814(6)	102
O4W–H4WB···O5	0.85	1.98	2.647(6)	135
O5W–H5WA···O5	0.85	2.04	2.693(6)	133
O5W–H5WB···O14	0.85	1.94	2.783(6)	176
O6W–H6WA···O4	0.85	2.18	2.941(6)	149
O6W–H6WA···O5	0.85	2.48	3.101(7)	131
O6W–H6WB···O14	0.85	2.06	2.808(6)	146
O7W–H7WA···N4	0.85	2.13	2.795(6)	135
O7W–H7WB···O2W	0.85	2.38	2.802(6)	111
O7W–H7WB···O7W	0.85	2.49	2.852(6)	107
O8W–H8WA···O14	0.85	2.55	3.192(18)	133
O8W–H8WB···O4W	0.85	2.58	2.98(2)	110

C3–H3A···O10	0.93	2.53	3.422(7)	162
C7–H7A···O14	0.97	2.36	3.312(7)	167
C11–H11A···O3	0.93	2.39	3.246(7)	152
C15–H15B···O2	0.97	2.60	3.384(7)	138

Symmetry code: A: –1+x, y, z B: 1+x, y, z

Table S3 Fluorescence intensity of the blank samples

n	ccpcTb in water	ccpcTb in methanol
1	1.82878E+06	1.13961E+06
2	1.82050E+06	1.14063E+06
3	1.83246E+06	1.13174E+06
4	1.84129E+06	1.12570E+06
5	1.84552E+06	1.13037E+06
6	1.83025E+06	1.13858E+06
7	1.82749E+06	1.12524E+06
8	1.84018E+06	1.13664E+06
9	1.81884E+06	1.12832E+06
10	1.82730E+06	1.12889E+06

Reference

[1] Bruker APEX2, v2014.5−0; Bruker AXS Inc: Madison, WI, 2007.

[2] Bruker. SAINT, v8.34A; Bruker AXS Inc: Madison, WI, 2013.

[3] Bruker. SADABS, Bruker AXS Inc: Madison, WI, 2014.

[4] SHELXTL, Software Reference Manual; Bruker, AXS, Inc: Madison, WI, 1997.

[5] G. Sheldrick, Acta Crystallogr. Sect. C: Cryst. Struct. Commun., 71(2015) 3.

[6] M. J. Frisch, G. W. Trucks, H. B. Schlegel, et al., Gaussian 09, Revision 8.0, Gaussian, Inc., Wallingford CT, 2009.